ORIGINAL PAPER



Prandtl-Tomlinson-Type Models for Coupled Molecular Sliding Friction: Chain-Length Dependence of Friction of Self-assembled Monolayers

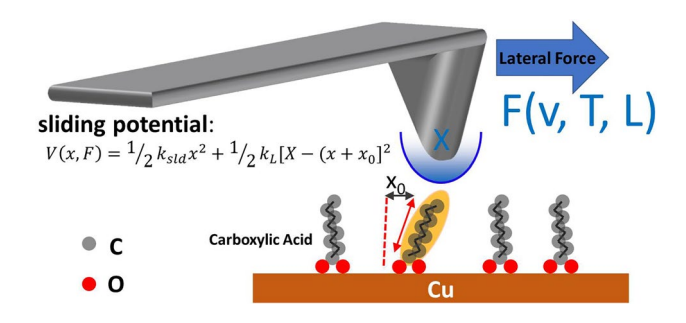
Kaiming Hou³ · Robert Bavisotto³ · Sergio Javier Manzi¹ · Eliseo Joaquín Perez¹ · Octavio Javier Furlong¹ · Peter Kotvis³ · Germaine Djuidje Kenmoe^{2,3} · Wilfred T. Tysoe³

Received: 21 February 2022 / Accepted: 28 April 2022 / Published online: 14 May 2022 © The Author(s), under exclusive licence to Springer Science+Business Media, LLC, part of Springer Nature 2022

Abstract

Previous work (Manzi et al. in Tribol Lett 69:147, 2021) proposed a tip-molecular interaction for calculating the friction of organic overlayers that consisted of a parabolic potential that extended to some cut-off distance when the energy reached a value of $E_{\rm sld}^0$, which represents an activation barrier for the detachment of the tip from the molecular terminus. A proposed advantage of such a potential was that it could be coupled to other degrees of freedom of the system. A method for accomplishing this is described here for the interaction between a tip and a compliant molecular chain to model the velocity, temperature, and chain-length dependences of the friction force. Analytical equations are derived for constant force sliding, such as in a ball-on-flat tribometer, and for compliant sliding, such as in an atomic force microscopy (AFM) experiment. The analytic models provided good fits to the chain-length dependence of the friction of carboxylate self-assembled monolayers (SAMs) on copper measured in an ultrahigh vacuum tribometer as part of this work and for alkyl thiolate SAMs on gold measured by an AFM taken from the literature. The results indicate that the commonly observed decrease in friction with increasing chain length has a component that is due to geometrical effects, as well as the possible participation of interchain van der Waals' interactions that are commonly invoked as being responsible for the friction reduction.

Graphical Abstract



Keywords Friction · Prandtl-Tomlinson model · Self-assembled monolayers · Friction modifiers

1 Introduction

Molecular-scale measurements of the velocity and temperature dependences of the friction of solid interfaces measured in an atomic force microscope (AFM) [1–4] are commonly analyzed using the Prandtl–Tomlinson (P–T) model [5, 6]. This assumes that friction occurs as atoms in the contact slide over a periodic (generally sinusoidal) potential,

Wilfred T. Tysoe wtt@uwm.edu

Extended author information available on the last page of the article



66 Page 2 of 11 Tribology Letters (2022) 70:66

where the energy is rapidly dissipated after surmounting the corresponding energy barrier. This theory has provided a fundamental understanding of the temperature and velocity dependences of sliding friction, as well as the experimentally observed atomic stick–slip behavior [2, 7–11]. The model rationalizes the logarithmic velocity variation in friction force, which increases with velocity, v, up to a point at which the external force causes the energy barrier to decrease to zero, after which the friction force becomes constant [6].

Similar velocity dependences have been observed for molecular adsorbates on surfaces, implying that similar P–T-type models might be expected to operate for molecular films. However, the behavior is likely to be more complex because both $ln(\nu)$ and more complex velocity dependences have been observed for adsorbed molecular layers [12–17]; in some cases, friction increases and then decreases as a function of velocity.

As a first step to analyzing the frictional properties of such organic adsorbates, we proposed a simple tip-molecular adsorbate interaction potential that is similar in shape to Morse [18] or Lennard-Jones potentials and which is consistent with the shapes of force-distance curves measured by AFM [19], where an initial attractive interaction can lead to a snap into contact and the presence of a pulloff force indicates that there is tip-surface interaction [20]. The proposed form of the sliding surface potential is shown in Fig. 1, where there is a parabolic variation in energy as a function of the sliding coordinate until a critical distance Δx^{\ddagger} is reached, at which the tip detaches and can move and attach to an adjacent site located at a distance a away. Thus, the periodicity of the adsorbates is taken to be equal toa. This potential is similar to those that have been used in Evans-Polanyi [21] models or Marcus

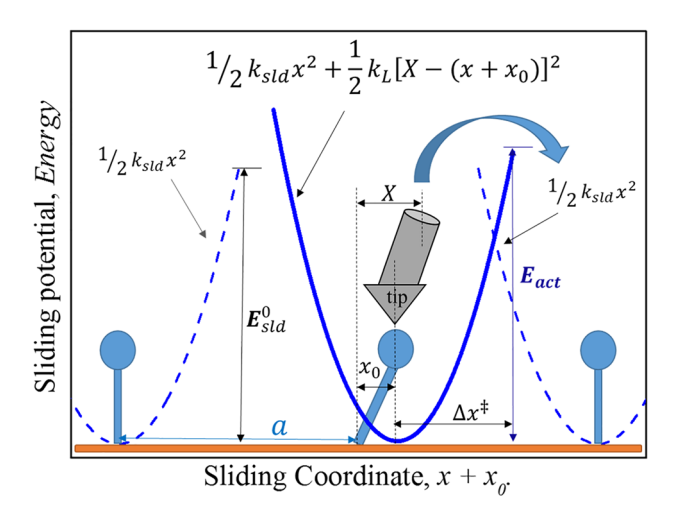


Fig. 1 Plot of the model's sliding potential used to describe the sliding of an AFM tip over an array of molecular adsorbates



theory [22]. The unperturbed adsorbate is defined at x = 0and has a minimum energy at this value, so that the sliding surface potential is expressed as $V_S(x) = \frac{1}{2}k_{\rm sld}x^2$, where $k_{\rm sld}$ is the corresponding force constant and is only valid while the tip is in contact with (attached to) the adsorbed species. It is also assumed that this interaction varies smoothly until reaching a sliding activation energy $E_{\rm sld}^0$ (Fig. 1, solid black line), that is, when the sliding coordinate reaches a value of Δx^{\ddagger} , so that $k_{\rm sld} = \frac{2E_{\rm sld}^0}{(\Delta x^{\ddagger})^2}$ and therefore the sliding surface potential is also given by: $V_{\rm S}(x) = E_{\rm sld}^0 \left(\frac{x}{\Delta x^{\ddagger}}\right)^2$. An analytical solution was given for this model without molecular tilting that was validated using kinetic Monte Carlo theory simulations, which were also able to delineate its limitations [20], which primarily occurred when both forward and reverse transitions were allowed to occur. One of the rationales for selecting this potential shape was that it could easily be coupled to other degrees of freedom of the system. The simplest example of a coupled system is a molecular adsorbate in which the potential $V_s(x)$ describes the interaction between an AFM tip and the terminus of an adsorbate that can also tilt under the influence of a lateral force. It is shown below how these potentials can be quite simply coupled to provide analytical formulae for the friction of self-assembled monolayer (SAM) adsorbates as a function of the length of the hydrocarbon chain.

Such molecular overlayers have been found to be stabilized by intermolecular van der Waals' interactions, which have been proposed to contribute to the change in friction force as a function of chain length [23]. However, no molecular-scale analytical models have been developed for SAM friction, except for an early one [24] that uses linear viscoelasticity theory [25–27] to describe the resonant properties of the film. However, as indicated above, SAM friction often increases linearly with ln(v) to reach a plateau at sufficiently high velocities, reminiscent of the behavior found for the P-T model for solid-solid sliding [9, 28–32] rather than resonant behavior. Self-assembled monolayers are model systems for so-called friction modifiers [33–37] so that SAM friction has been extensively investigated. The friction force is found to decrease with the length of the hydrocarbon chain, so that friction modifiers in lubricants generally consist of long-chain fatty acids [33, 34, 38].

A molecular-scale P-T model of SAM friction will provide a basis for disentangling the effects that contribute to their friction and facilitate the ultimate design of more effective friction modifiers. In this work, a molecular P-T model is developed both for constant force sliding, such as that which occurs in a ball-on-flat tribometer, and for compliant sliding in an AFM. To test the theoretical

Tribology Letters (2022) 70:66 Page 3 of 11 **6**

predictions from the model developed below, constant force sliding experiments are carried out for carboxylic acids adsorbed on a copper substrates with different alkyl chain lengths, where they deprotonate to form adsorbed carboxylates [39–41]. Their surface chemistry has been thoroughly investigated because carboxylates are important intermediates in several catalytic reactions, e.g., hydrogen generation, alcohol synthesis, and the methanation of CO and CO₂ [42-45]. The carboxylate can bind tightly to clean metal surfaces in a bidentate configuration with two chemically equivalent oxygen atoms [46–49] to form close-packed carboxylate SAMs. Due to their high degree of order and their well-defined molecular thickness, SAMs of carboxylic acids provide an ideal model system for understanding interfacial properties and boundary lubrication at a molecular level [50–53]. We previously investigated the surface reactivity and tribochemistry of acetic, octanoic, and 7-octenoic acids [39, 41, 54, 55] on copper, and similar tribological studies have been carried out for alkanethiols and alkyl silanes, which show chainlength dependences such that longer chain molecules lead to lower friction forces [12, 23, 56–60].

The prediction of the P–T model applied to SAMs is tested in this work for a homologous series of carboxylates adsorbed on a copper substrate, where the friction is measured in an ultrahigh vacuum (UHV) tribometer in a ball-on-flat configuration, and the nature of the adsorbates is characterized using Auger and reflection–absorption infrared spectroscopies (RAIRS) [39, 40, 55, 61]. The theory is also compared with the results of nanoscale AFM experiments carried out using a compliant cantilever to measure the length dependence of SAM friction for alkyl thiolates on gold [23, 62].

2 Experimental Methods

Experiments were carried out in UHV chambers operating at pressures of $\sim 2.0 \times 10^{-10}$ Torr after bakeout. Ball-on-flat friction measurements were carried out in a UHV chamber, which has been described in detail elsewhere [63]. The chamber was equipped with a UHV-compatible tribometer, which simultaneously measures normal load, lateral force, and the electrical contact resistance between the tip and the substrate. All measurements were made using a sliding speed of $\sim 4 \times 10^{-3}$ m/s at a normal load of 0.44 N. Previous work has shown that the maximum interfacial temperature rise for a copper sample under these conditions is much lower than 1 K [64]. The spherical pin ($\sim 1.27 \times 10^{-2}$ m diameter) was made from tungsten carbide containing some cobalt binder and could be heated by electron bombardment in vacuo or by argon ion bombardment, in order to clean it; for the experiments reported here, it was cleaned by heating.

The pin was attached to an arm with attached strain gauges to enable the normal and lateral forces to be measured. The arm was mounted to a rotatable Conflat flange to allow the pin to be rotated to face a cylindrical mirror analyzer (CMA) to enable Auger spectra of both the pin surface and the copper sample to be obtained [65].

Infrared spectra were collected using a Bruker Vertex 70 infrared spectrometer using a liquid nitrogen cooled, mercury cadmium telluride detector [66]. The complete light path was enclosed and purged with dry CO₂-free air, and spectra were collected for 1000 scans at 4 cm⁻¹ resolution.

The copper foil was prepared by mechanical polishing using sandpapers of increasing grit size until no visible scratches were observed. This was followed by polishing using polycrystalline diamond paste until a visibly smooth surface was seen under a microscope. The samples were mounted in UHV to a precision x, y, and z manipulator for measuring the elemental profiles across a rubbed region of the sample. The copper foil sample was cleaned using a standard procedure consisting of cycles of Ar^+ bombardment with subsequent annealing to 850 K for 10 min. Ar^+ bombardment was performed at a background gas pressure of $\sim 5.0 \times 10^{-5}$ Torr at a 1 kV potential, while maintaining a $\sim 2 \mu A$ sample current.

The propionic acid (Sigma-Aldrich, \geq 90 purity), butanoic acid (Sigma -Aldrich, \geq 99.0 purity), pentanoic acid (Sigma -Aldrich, \geq 98.0 purity), hexanoic acid (Sigma -Aldrich, \geq 99% purity), heptanoic acid (Sigma-Aldrich, \geq 99.0% purity) ,and octanoic acid (Sigma-Aldrich, \geq 98.0% purity) were transferred to glass bottles and attached to the gas-handling system of the vacuum chamber, where they were subjected to several freeze–pump–thaw cycles.

3 Analytical Prandtl-Tomlinson Model for Constant Force Sliding

The Prandtl–Tomlinson model is analyzed for a surface potential $V_{\rm S}(x)$ of a counterface or tip interacting with the terminus of a hydrocarbon coupled to a tilting alkyl chain of length l as illustrated in Fig. 2, where the molecule is able to tilt through some (small) angle θ , with a tilting force constant k_{θ} . This gives rise to a harmonic potential due to tilting given by $V_{\rm t}=1/2k_{\theta}\theta^2$, where, to first order, k_{θ} will not depend strongly on the length of the chain and thus neglects the influence of interchain interactions. For small tilt angles, $\theta \approx x_0/l$, so that $V_{\rm t}=1/2\frac{k_{\theta}}{l^2}x_0^2$, so that $V_{\rm t}=1/2k_{\rm t}x_0^2$ and the force constant $k_{\rm t}$ are given by $k_{\rm t}=k_{\theta}/l^2$. In the case of an alkyl chain, the length of the carbonaceous chain depends on the number of carbon atoms n in the chain and can be approximated as $\sim d_{\rm cc}(n-1)$, where $d_{\rm cc}$ is the projected distance between carbon atoms of the carbon–carbon bond.



66 Page 4 of 11 Tribology Letters (2022) 70:66

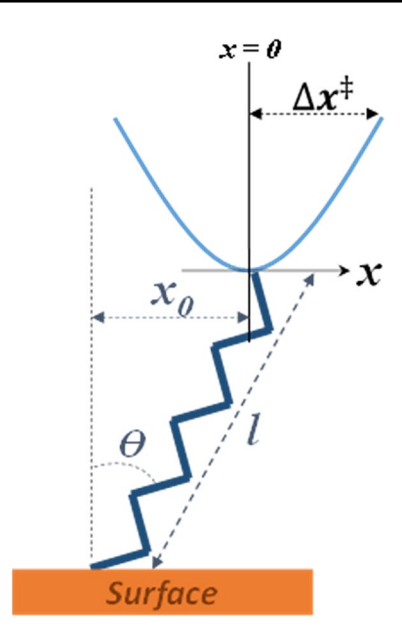


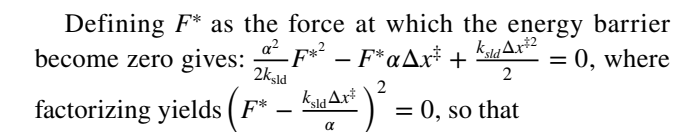
Fig. 2 Schematic depiction of the coupled adsorbate system used to analyze self-assembled monolayer friction

A tip slides over the overlayer and the interaction is described by the molecular sliding potential: $V_{\rm S}(x) = \frac{1}{2}k_{\rm sld}x^2 = E_{\rm sld}^0\left(\frac{x}{\Delta x^3}\right)^2$ and is anticipated to be constant for a series of SAMs (carboxylic acids or thiolates) with identical terminal groups.

This system can be described by two coupled springs, but the following analysis could easily be extended to more complex systems. The total displacement caused by the applied force is $x + x_0$ and the net force is zero at the junction between the two springs so that $k_{\rm sld}x = k_{\rm t}x_0$, where x_0 is the displacement of the terminus of the molecule from its equilibrium position (see Fig. 2) to give $x_0 = \frac{k_{\rm sld}}{k_{\rm t}}x$. The total potential for constant force sliding is given by $V(x,x_0,F) = 1/2k_{\rm sld}$ $x^2 - F(x + x_0)$, where F is the applied force (measured for ball-on-flat sliding in the UHV tribometer). Substituting for x_0 gives $V(x,F) = 1/2k_{\rm sld}x^2 - F\alpha x$, where $\alpha = \left(1 + \frac{k_{\rm sld}}{k_{\rm t}}\right)$, to illustrate how the previous analysis for molecular sliding can easily be extended to coupled systems.

The minimum in this potential is given by: $\frac{\partial V}{\partial x}\Big|_F = k_{\rm sld}x - F\alpha = 0$, so that $x_{min} = F\alpha/k_{\rm sld}$ to give $V_{min} = -\frac{1}{2}\frac{\alpha^2}{k_{\rm sld}}F^2$. As shown previously [20], V_{max} is obtained when $x = \Delta x^{\ddagger}$ and gives $V_{\rm max} = 1/2 \; k_{\rm sld} \Delta x^{\ddagger 2} - F\alpha \Delta x^{\ddagger}$. This yields a force-dependent activation energy $E_{\rm act}(F) = V_{max} - V_{min}$ to give:

$$E_{\rm act}(F) = \frac{k_{\rm sld}}{2} \Delta x^{\ddagger 2} - F \alpha \Delta x^{\ddagger} + \frac{\alpha^2}{2k_{\rm sld}} F^2. \tag{1}$$



$$F^* = \frac{k_{\rm sld} \Delta x^{\ddagger}}{\alpha}.$$
 (2)

A similar factorization of Eq. 1 gives:

$$(F) = \frac{\alpha^2}{2k_{\rm sld}}(F^* - F)^2,\tag{3}$$

so that the energy barrier tends to zero as the lateral force tends to F^* . This can be used to calculate the velocity and temperature dependences of sliding friction by taking the rate constant for the transition over the energy barrier between one molecular terminus and the next as $k = A \exp\left(-\frac{E_{act}(F)}{k_BT}\right)$, where A is a pre-exponential factor, k_B is the Boltzmann constant, and T is the temperature. If the sliding speed is v and the periodicity of the adsorbed monolayer is a, then the time for each transition is given by $\tau = a/v$, so that [67, 68] $k = \frac{1}{\tau} = \frac{v}{a} = Aexp\left(-\frac{E_{act}(F)}{k_BT}\right)$. This gives $ln\left(\frac{v}{Aa}\right) = -\frac{E_{act}(F)}{k_BT}$. Putting $Aa = v_0$ and substituting from Eq. 3 gives:

$$(F^* - F)^2 = \frac{2k_{\rm sld}k_{\rm B}T}{\alpha^2} \ln\left(\frac{v_0}{v}\right). \tag{4}$$

At a constant temperature and sliding velocity $2k_{\rm sld}k_{\rm B}Tln\left(\frac{v_0}{v}\right)=B^2$ is constant, while α depends on the chain length l, so that $F^*-F=\pm\frac{B}{\alpha}$. Since F^* is the maximum force, $F^*-F>0$, so that $\frac{B}{\alpha}>0$ and thus $F=F^*-\frac{B}{\alpha}$. This is in accord with the commonly observed temperature and velocity dependences [5, 9, 28–31], where an increase in temperature leads to an increase in B and therefore a decrease in B, while an increase in B to decrease and thus an increase in B. Substituting from Eq. 2 for B gives:

$$F(T, v, l) = \frac{1}{\alpha} \left(k_{\rm sld} \Delta x^{\ddagger} - B \right), \tag{5}$$

where $\alpha = \left(1 + \frac{k_{\rm sld}}{k_{\rm t}}\right)$ and $k_{\rm t}$ are expected to depend on the chain length as $k_{\rm t} = \frac{k_{\rm \theta}}{l^2}$, so that $\alpha = \left(1 + \frac{k_{\rm sld}}{k_{\rm \theta}}l^2\right)$. Note that as l increases, α become larger and the friction decreases as found experimentally below.

4 Analytical Prandtl-Tomlinson Model for Compliant Sliding

This analysis can be extended to describe the compliant sliding of an AFM tip, where P–T-like behavior has been seen in which the friction force rises with the logarithm of



Tribology Letters (2022) 70:66 Page 5 of 11 **6**

the velocity and then reaches a plateau [12]. In this case, the compliant potential is given by:

$$V(x, x_0, X) = \frac{1}{2} k_{\text{sld}} x^2 + \frac{1}{2} k_{\text{L}} (X - (x + x_0))^2, \tag{6}$$

where $k_{\rm L}$ is the cantilever force constant, X is the position of the cantilever, and, as above, $x + x_0 = \alpha x$. Thus,

$$V(x,X) = \frac{1}{2}k_{\rm sld}x^2 + \frac{1}{2}k_{\rm L}(X - \alpha x)^2.$$
 (7)

Writing $k_{\rm L}/k_{\rm sld} = K$ and evaluating $\frac{\partial V}{\partial x}\Big|_{X} = 0$ yields:

$$x_{\min} = \frac{\alpha K}{1 + \alpha^2 K} X. \tag{8}$$

Substituting into Eq. 7 gives $V_{min} = \frac{1}{2} \left(\frac{k_{sld}K}{1 + \alpha^2 K} \right) X^2$. The force depends on X as $F = k_L \left(X - \alpha x_{min} \right)$ so that $F = \left(\frac{k_{sld}K}{1 + \alpha^2 K} \right) X$.

Furthermore, V_{max} occurs when $x = \Delta x^{\ddagger}$, so that Eq. 7 becomes $V_{max} = 1/2k_{\rm sld}\Delta x^{\ddagger 2} + 1/2k_{\rm L} \left(X - \alpha \Delta x^{\ddagger}\right)^2$ and the activation energy can be calculated as a function of X from the difference between the maximum and minimum energies, which, with some manipulation yields:

$$E_{\text{act}}(X) = \frac{k_{\text{sld}}}{2} \left(1 + \alpha^2 K \right) \left[\Delta x^{\ddagger} - \left(\frac{\alpha K}{1 + \alpha^2 K} \right) X \right]^2. \tag{9}$$

Substituting for *X* gives the force-dependent activation energy as:

$$E_{\text{act}}(F) = \frac{1}{2k_{\text{old}}} \alpha^2 (1 + \alpha^2 K) (F^* - F)^2, \tag{10}$$

where, as found above, $F^* = k_{\rm sld} \Delta x^{\ddagger}/\alpha$ and is again the force at which the activation barrier decreases to zero. As has been shown previously for the Prandtl–Tomlinson model based on the principle of detailed balance [2, 4], the probability of a forward transition is governed by: $\frac{dP(E_{\rm act})}{dt} = -P(E_{\rm act})A\exp\left(-\frac{E_{\rm act}(F)}{k_{\rm B}T}\right).$ This can be converted into an equation that depends on F from $\frac{dP(F)}{dt} = \frac{dP(F)}{dF}\frac{dF}{dt}.$ Since the cantilever moves at a velocity v, then $F = \left(\frac{k_{\rm sld}K}{1+\alpha^2K}\right)vt.$ The maximum rate is given by $\frac{d^2P(F)}{dF^2} = 0 \text{ to yield: } \frac{1}{k_{\rm B}T}\frac{dE_{\rm act}(F)}{dF} + \frac{(1+\alpha^2K)A}{k_{\rm sld}Kv}\exp\left(-\frac{E_{\rm act}(F)}{k_{\rm B}T}\right) = 0,$ where v is the sliding velocity, to give:

$$\frac{\mathrm{d}E_{\mathrm{act}}(F)}{\mathrm{d}F} = -\frac{\left(1 + \alpha^2 K\right) A k_{\mathrm{B}} T}{k_{\mathrm{sld}} K \nu} \exp\left(-\frac{E_{\mathrm{act}}(F)}{k_{\mathrm{B}} T}\right). \tag{11}$$

From Eq. 10, the first derivative is as follows:

$$\frac{\mathrm{d}E_{\mathrm{act}}(F)}{\mathrm{d}F} = -\frac{\alpha^2}{k_{\mathrm{eld}}} (1 + \alpha^2 K)(F^* - F). \tag{12}$$

Finally, equating Eqns. 11 and 12, and rearranging, gives:

$$\frac{1}{\beta k_{\rm p} T} (F^* - F)^2 = \ln\left(\frac{v_0}{v}\right) - \ln\left(F^* - F\right),\tag{13}$$

where
$$v_0 = \frac{Ak_BT}{K\alpha^2}$$
 and $\beta = \frac{2k_{\text{sld}}}{\alpha^2(1+\alpha^2K)}$.

5 Results

These predictions are tested for carboxylate SAMs on copper measured in a UHV tribometer, where the order and nature of the films are gauged using RAIRS from the width of the asymmetric methylene stretching vibration. In addition, the variation in friction with chain length is compared with theory using previous measurements for alkyl thiolate SAMs on gold.

5.1 Infrared and Auger Analyses of Alkyl Carboxylates on Copper

The Auger spectra of the carboxylate monolayers on copper were collected in the UHV tribometer immediately before measuring the friction coefficient for ball-on-flat sliding without removing the sample from the UHV chamber. The resulting plot of the peak-to-peak intensity of the carbon KLL Auger signal ratioed to the copper KLL peak-to-peak intensity at 921 eV kinetic energy is shown in Fig. 3A. The results are analyzed by approximating the total length of the n-carbon carboxylate chain as $l \sim d_{coo} + d_{cc}(n-1)$, where d_{coo} is the contribution from the carboxylate anchoring group, d_{cc} is the projected carbon-carbon bond length along the chain, and n is the number of carbon atoms in the alkyl chain. If $d_{coo} \cong d_{cc}$, the length of the n-carbon chain is $l \sim d_{CC}n$, and the intensity ratio is quite straightforwardly calculated as [69–72]:

$$\frac{I_{\rm C}}{I_{\rm Cu}} = N \frac{\left(1 - \exp\left(-\frac{d_{\rm cc}}{\lambda_{\rm c}}n\right)\right)}{\exp\left(-\frac{d_{\rm cc}}{\lambda_{\rm c}^{\rm Cu}}n\right)},\tag{14}$$

where the inelastic mean-free path parameters λ are described in the Supplementary Information section. This function is fitted to the experimental data in Fig. 3B, showing a very good agreement with $N=0.37\pm0.03$, $\frac{d_{cc}}{\lambda_C}=0.39\pm0.03$, and $\frac{d_{cc}}{\lambda_C^{Cu}}=0.040\pm0.006$.

A similar analysis for the oxygen signal is shown in Fig. 3B, which similarly ratios the O KLL signal to the intensity of the copper signal for various alkyl carboxylate films. Because the oxygen atoms from the carboxylate groups are buried below the carbon-containing alkyl film, the signals are much smaller than those from the carbon



66 Page 6 of 11 Tribology Letters (2022) 70:66

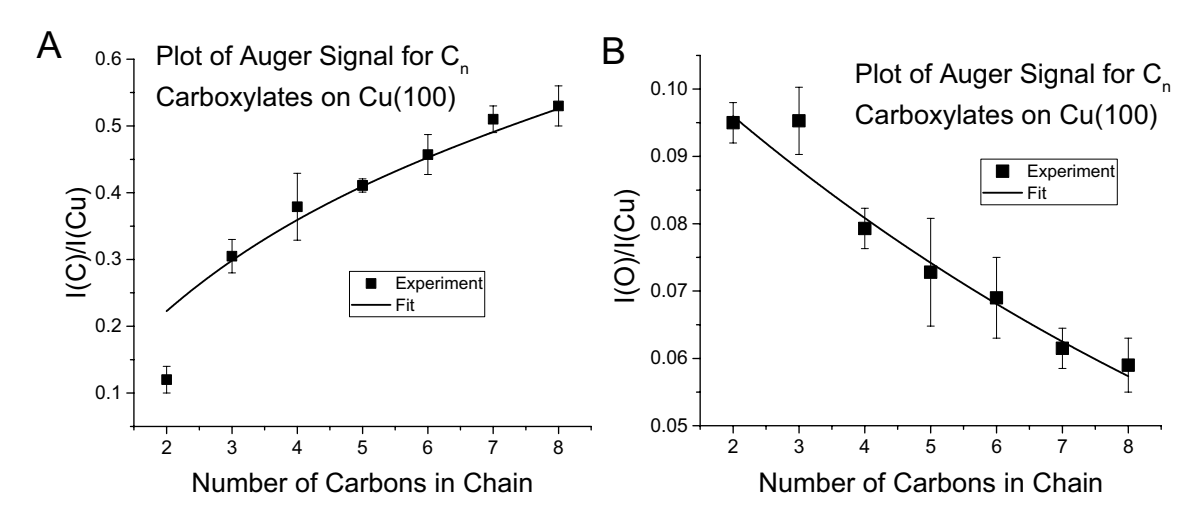


Fig. 3 A Plot of the peak-to-peak C KLL Auger signal ratioed to the Cu LMM Auger signal for saturated overlayers of carboxylates with C_n alkyl chains as a function of the number of carbons in the chain. **B**

Plot of the peak-to-peak O KLL Auger signal ratioed to the Cu LMM Auger signal for saturated overlayers of carboxylates as in A

spectrum; nevertheless, the results can be fit using a similar analysis and gives:

$$\frac{I_{\rm C}}{I_{\rm Cu}} = N \exp\left(-\left(\frac{1}{\lambda_{\rm C}^{\rm O}} - \frac{1}{\lambda_{\rm C}^{\rm Cu}}\right) d_{\rm cc} n\right),\tag{15}$$

where the meanings of the symbols are given in the Sup-

plementary Information section. The fit to this formulae is shown in Fig. 3B and agrees well with the experimental data with $N=0.114\pm0.003$ and $\left(\frac{1}{\lambda_C^0}-\frac{1}{\lambda_C^{Cu}}\right)d_{\rm cc}=0.086\pm0.007$. Using that value of $\frac{d_{\rm cc}}{\lambda_C^{Cu}}$ measured above gives $\frac{d_{\rm cc}}{\lambda_C^0}\sim0.12$. These results are consistent with the proposed structural model in which the film is bound by adsorbed carboxylate groups and suggest that all the overlayers have the same saturation coverages.

The infrared spectra [73–76] of SAMs have been used to gauge their order and packing density [12]. In particular, the vibrational frequency of the asymmetric methylene stretching mode $(v_a(CH_2))$ has been found to shift from ~2918 to 2924 cm⁻¹ as the films become less ordered. However, the stretching modes for carboxylates in copper are relatively weak, while the bending modes are easier to detect, especially for the shorter-chain adsorbates. Figure 4 shows the infrared spectra of a multilayer of octanoic acid adsorbed on copper at 92 K and heated to various temperatures, where the annealing temperature is displayed adjacent to the corresponding spectrum. Assignments of the C-H stretching modes are given in the figure and agree well with those in the literature [73]. In particular, the methylene asymmetric stretching mode for a film formed at 92 K has a frequency of 2920 cm⁻¹, somewhat lower than for a completely disordered (liquid) film of 2924 cm⁻¹. Heating to 203 K causes

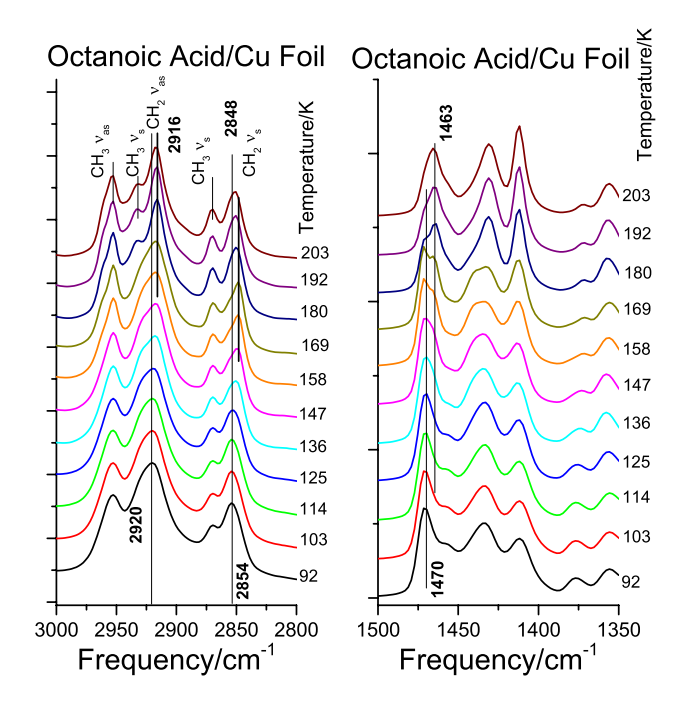


Fig. 4 Infrared spectra of octanoic acid adsorbed on copper at 92 K and annealed to various temperatures, where the annealing temperatures are indicated adjacent to the corresponding spectrum. The C–H stretching region is shown in the left-hand spectra and the carboxylate C–H bending modes are shown in the right-hand spectra

this peak to shift to $2916~\rm cm^{-1}$, consistent with the film ordering and shifting to the frequency in the solid. The C–H bending region is also displayed in Fig. 4 and shows a shift in the $1470~\rm cm^{-1}$ peak to $1463~\rm cm^{-1}$ on heating to $\sim 203~\rm K$, consistent to a more disordered film becoming more ordered as the film is heated. This indicates that the bending modes



Tribology Letters (2022) 70:66 Page 7 of 11 **66**

can be used to gauge the order of the carboxylate monolayer on copper. The RAIRS spectra in the C-H bending region for the films for which the friction was measured are displayed in Figure S1 in the Supplementary Information section. The profiles of the asymmetric methylene stretching features were fit to Gaussian functions to enable the peak widths and positions to be estimated; the results are plotted versus the number of carbon atoms in the alkyl chain of the SAMs on copper in Fig. 5. This indicates that the order of the alkyl chains increases as the length of the chain increases. However, as shown below, the friction decreases with increasing chain length in accord with the above coupled P-T model that does not include intermolecular interactions. Comparisons are made between theory and experiment, both for constant force sliding for the measurements performed in the UHV tribometer for carboxylates adsorbed on a copper substrate as a function of chain length, as well as for previous AFM measurements for SAMs on gold.

5.2 Comparison with Experiment for Constant Force Sliding

Figure 6 shows a plot of the friction coefficient of a series of alkyl carboxylates with different chain lengths adsorbed on clean copper measured using a UHV tribometer. This shows a decrease in friction with chain length which can be approximated as $l \sim d_{\rm cc} n$, so that Eq. 5 becomes $F = F_0/(1 + rn^2)$, where $F_0 = k_{\rm sld} \Delta x^\ddagger - B$ and $r = \frac{k_{\rm sld}}{k_{\theta}} d_{\rm cc}^2$. Dividing by the constant normal force gives $\mu = \mu_0/(1 + rn^2)$, where μ is the friction coefficient. This curve is shown plotted with the experimental data in Fig. 6 and shows reasonable agreement

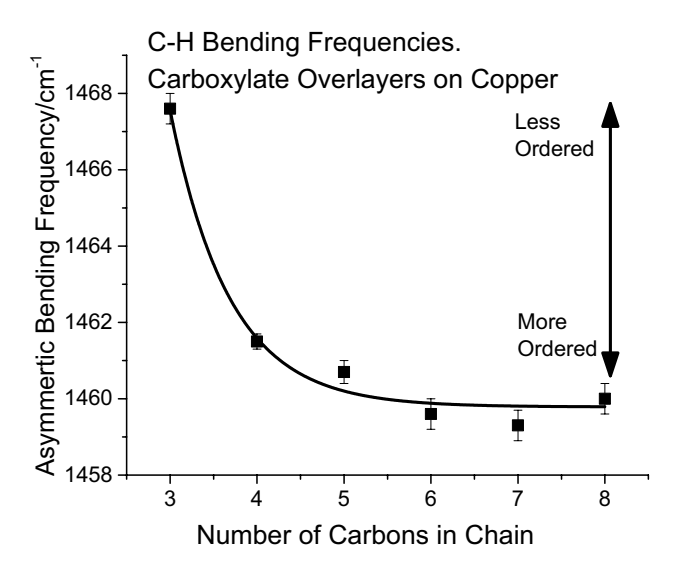


Fig. 5 Plot of the frequency of the asymmetric methylene bending mode $(\delta_{as}(CH_2))$ versus the number of carbon atoms in the alkyl chains of the carboxylates adsorbed on copper

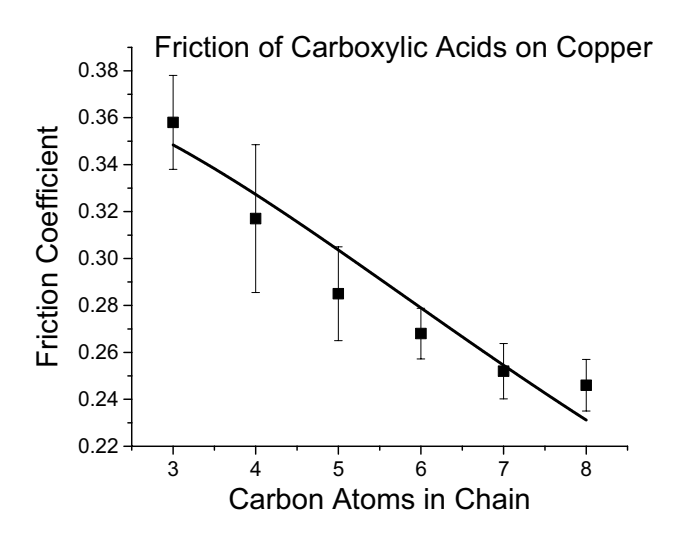


Fig. 6 Plot of the friction coefficient versus the length of the alkyl chain for a number of alkyl carboxylates adsorbed on a clean copper substrate measured in a UHV tribometer. The line represents a fit to the formula in Eq. 4

with experiment, giving $\mu_0 = 0.378 \pm 0.017$ and $r = \left(\frac{k_{\rm sld}}{k_{\rm g}}\right) d_{\rm cc}^2 = 0.010 \pm 0.002$. These results suggest that the simple molecular P–T model for coupled harmonic potentials provides adequate agreement with experiment, although there are deviations from the experiment that may suggest that changes in the extent of ordering (Fig. 5) do play a role.

5.3 Comparison with Experiment for Compliant Sliding

Analogous results are shown in Fig. 7 for the relative friction forces of alkyl thiolates on gold from two different research groups [12, 23]. The experiments from Porter et al. used triangular Si₃N₄ cantilevers at a sliding speed of 1 μm/s and measured the lateral force f as a function of the normal force F_N , finding a linear dependence: $f = \alpha F_N + f_0$. The friction was obtained from the slopes, α , and the normalized friction is plotted versus the number of carbons in the alkyl chain in Fig. 7 (black circle). Similar data were obtained by the Leggett group (black square), although the experimental conditions were not specified; the normalized results are also displayed in Fig. 7 and, except for the divergence for longer chains, the data are in good agreement. The general behavior with chain length is similar to that for constant force sliding (Fig. 6), where the friction force decreases with increasing chain length. The velocity and temperature dependences of friction force for chains with different lengths are given in Eq. 13, but does not yield a simple analytical force dependence. Equation 13 can be simplified by assuming that $F \ll F^*$, so that $(F^* - F)^2 = F^{*2} \left(1 - 2 \frac{F}{F^*} \right)$. Expanding $\ln(F^* - F) = \ln(F^*)$ $-ln\left(1-\frac{F}{F^*}\right)$ to first order simplifies Eq. 13 to give



66 Page 8 of 11 Tribology Letters (2022) 70:66

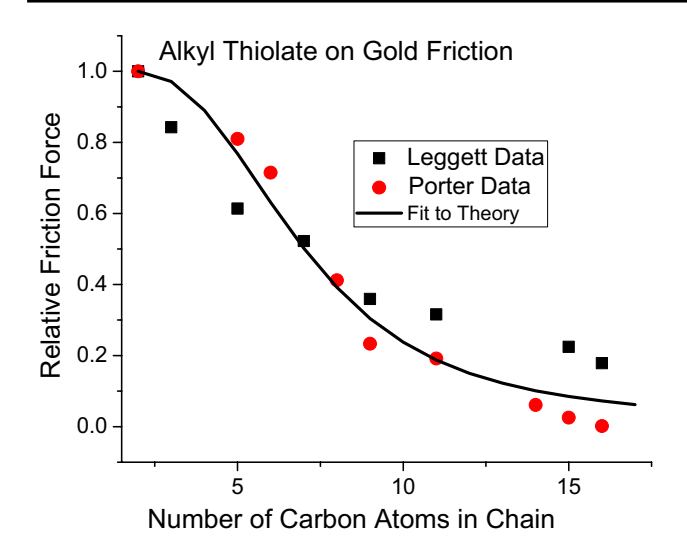


Fig. 7 Plot of the friction coefficient versus the length of the alkyl chain for a number of alkyl thiolates adsorbed on a clean gold substrate measured in an atomic force microscope showing data from Leggett et al. [12] and Porter et al. [23]. The line shows a fit to the coupled P–T model

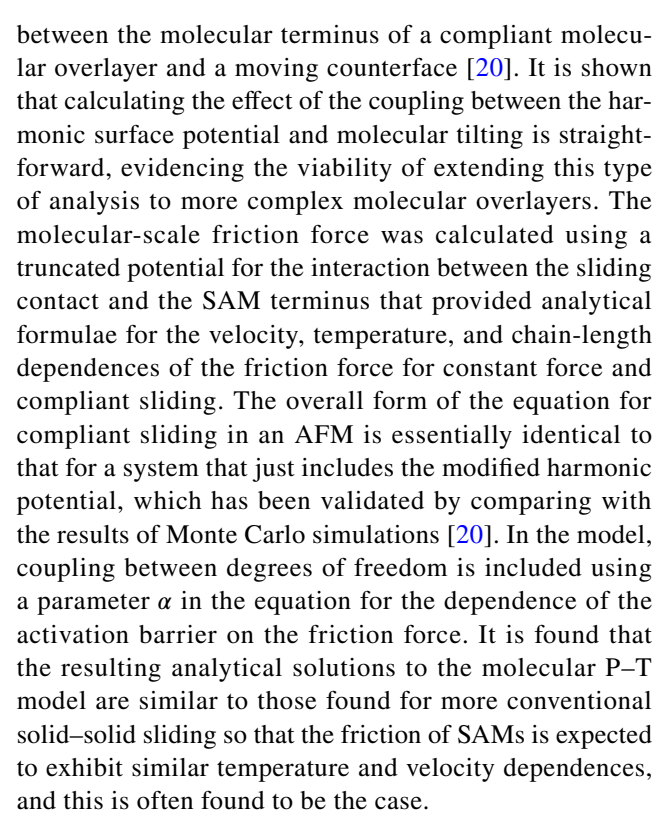
 $\frac{1}{\beta k_{\rm B}T} F^{*2} \left(1 - 2 \frac{F}{F^*} \right) = ln \left(\frac{v_0}{vF^*} \right) + \frac{F}{F^*}.$ This can now be separated to give an explicit equation for *F* as:

$$F = \frac{F^*}{2F^{*2} + \beta k_{\rm B}T} \left[F^{*2} - \beta k_{\rm B}T \ln \left(\frac{v_0}{F^*v} \right) \right]. \tag{16} \label{eq:16}$$

As shown above, some of these parameters depend on the chain length through $\alpha=1+\frac{k_{\rm sld}}{k_{\theta}}l^2$, so that $F^*=\frac{k_{\rm sld}\Delta x^*}{\alpha}=\frac{F_0^*}{\alpha}$, $\beta=\frac{2k_{\rm sld}}{\alpha^2(1+K\alpha^2)}=\frac{\beta_0}{\alpha^2(1+K\alpha^2)}$, and $v_0=\frac{Ak_{\rm B}T}{K\alpha^2}$. As above, we write $r=\left(\frac{k_{\rm sld}}{k_{\theta}}\right)d_{\rm cc}^2$. The fit is carried out numerically by calculating the force as a function of n and normalizing the result to the value when the number of carbons in the chain equals 2, in order to correspond to the experiment data in Fig. 7, and the parameters are adjusted manually to produce the best agreement with the experimental results to yield $F_0^*=0.4\pm0.1$, $K=1.0\pm0.1$, $V=2.9\pm0.1$, $r=\left(\frac{k_{\rm sld}}{k_{\theta}}\right)d_{\rm cc}^2=0.037\pm0.002$, and $\beta_0=1.1\pm0.1$. The agreement between the experiment and the prediction from Eq. 16 is good. In particular, the values of r for constant force sliding (0.010 ± 0.002) is quite close to that found for both SAMs measured by AFM (0.037 ± 0.002) despite having been obtained for different SAMs and using very different tribological measurements.

6 Discussion

An analytical Prandtl-Tomlinson molecular sliding model is developed for a coupled system, which consists of a truncated harmonic potential that describes the interaction



The friction coefficients of self-assembled monolayers formed in vacuum on a copper substrate from carboxylic acid adsorption, as well as the friction forces of alkyl thiolate self-assembled monolayers formed from solution on gold, are in good agreement with the predicted chainlength dependence from the analytical-coupled molecular P–T model presented in this work. Note that both SAMs show changes in their infrared spectra that indicate that the films become more ordered due to increasing interchain van der Waals' interactions as the length of the alkyl chain increases, although the frictional behavior can be analyzed without invoking these effects.

The extent to which each of these effects play in the overall energy dissipation processes occurring in self-assembled monolayers at sliding interfaces still remains to be determined. Nevertheless, such a fundamental understanding will be central to designing effective friction modifier additives to lubricants. Molecular dynamics simulations have been carried out on model SAMs [77], but we are not aware of any that specifically model the friction force as a function of chain length for a homologous series of adsorbates. Simulations do reveal the formation of gauche defects in the chain during sliding [78, 79] and have shown that the friction does depend on the SAM packing density where tightly packed layers exhibit significantly lower friction than the loosely packed monolayer at high loads [80].



Tribology Letters (2022) 70:66 Page 9 of 11 **6**

7 Conclusion

Previous work showed how the interaction between and AFM tip and the terminus of a molecule could be modeled using a simplified interaction potential consisting of a truncated parabola that extends to some cut-off distance designated as Δx^{\ddagger} at which the energy reaches a value of $E^0_{\rm std}$ that corresponds to an activation barrier for the detachment of the tip from the molecular terminus [20]. An analytical Prandtl-Tomlinson-type model was previously developed for this model potential and its applicability and limitations were investigated using kinetic Monte Carlo methods. A rational for using a harmonic form of the potential was the facility with which it could be coupled to other degrees of freedom of the system. Strategies for accomplishing this are outlined in the present work for the truncated potential coupled to a harmonic tilting of a chain to mimic the friction of a self-assembled monolayer. The approach is illustrated both for constant force sliding, such as encountered in a traditional ball-on-flat tribometer, and for compliant sliding, such as in an atomic force microscope. These analyses result in analytical formulae for the dependence of the friction force on velocity, temperature, and the length of the carbon chain. The predictions from the model were compared with experimental alkyl chain-length dependences, obtaining good agreement with the experimentally observed decrease in friction force with increasing chain length. The model assumes that there are no interchain interactions and the agreement between theory and experiment implies that the effect may be purely geometric where longer alkyl chains result in less elastic energy being stored as the length of the chain increases, so that less energy is dissipated as the tip moves from one site to the adjacent one, leading to a lower friction force. This model differs from the conventional view that the reduction in friction with increasing chain length originates from a stiffening of the SAM due to interchain van der Waals' interactions. Infrared spectroscopic analysis of the films used in this work for constant force sliding experiments, as well as for experiments for compliant sliding in an AFM show that interchain interactions do occur and are stronger for longer chains. However, it does appear that these effects may not be dominant in controlling the decrease in friction with increasing chain length.

Supplementary Information The online version contains supplementary material available at https://doi.org/10.1007/s11249-022-01609-z.

Acknowledgements We gratefully acknowledge the Civil, Mechanical and Manufacturing Innovation (CMMI) Division of the National Science Foundation under grant number 2020525 for support of this work. GDK thanks the Fulbright Foundation for support of this work. KH acknowledges support from the China Scholarship Council.

Author Contributions All authors contributed equally to this work.

Funding Division of Civil, Mechanical and Manufacturing Innovation (2020525) and Distinguished International Students Scholarship.

Data Availability Data are available in article or as Supplementary Material.

Declarations

Conflict of interest The authors have not disclosed any competing interests.

Ethical Approval All ethical responsibilities were respected by the authors

References

- Carpick, R.W., Salmeron, M.: Scratching the surface: fundamental investigations of tribology with atomic force microscopy. Chem. Rev. 97, 1163–1194 (1997)
- Gnecco, E., Bennewitz, R., Gyalog, T., Loppacher, C., Bammerlin, M., Meyer, E., et al.: Velocity dependence of atomic friction. Phys. Rev. Lett. 84, 1172–1175 (2000)
- Gnecco, E., Bennewitz, R., Gyalog, T., Meyer, E.: Friction experiments on the nanometre scale. J. Phys. Condens. Matter. 13, R619–R642 (2001)
- Bennewitz, R., Gnecco, E., Gyalog, T., Meyer, E.: Atomic friction studies on well-defined surfaces. Tribol. Lett. 10, 51–56 (2001)
- Tomlinson, G.A.: A Molecular Theory of Friction. Phil Mag 7, 905 (1929)
- Prandtl, L.: Ein Gedankenmodell zur kinetischen Theorie der festen Körper. Z. Angew. Math. Mech. 8, 85 (1928)
- Sang, Y., Dube, M., Grant, M.: Thermal effects on atomic friction. Phys. Rev. Lett. 87, 174301 (2001)
- 8. Riedo, E., Gnecco, E., Bennewitz, R., Meyer, E., Brune, H.: Interaction potential and hopping dynamics governing sliding friction. Phys. Rev. Lett. **91**, 084502 (2003)
- Fusco, C., Fasolino, A.: Velocity dependence of atomic-scale friction: A comparative study of the one- and two-dimensional Tomlinson model. Phys. Rev. B 71, 045413 (2005)
- Socoliuc, A., Bennewitz, R., Gnecco, E., Meyer, E.: Transition from stick-slip to continuous sliding in atomic friction: entering a new regime of ultralow friction. Phys. Rev. Lett. 92, 134301 (2004)
- Porto, M., Zaloj, V., Urbakh, M., Klafter, J.: Macroscopic versus microscopic description of friction: from Tomlinson model to shearons. Tribol. Lett. 9, 45–54 (2000)
- Brewer, N.J., Beake, B.D., Leggett, G.J.: Friction force microscopy of self-assembled monolayers: influence of adsorbate alkyl chain length, terminal group chemistry, and scan velocity. Langmuir 17, 1970–1974 (2001)
- Bliznyuk, V.N., Everson, M.P., Tsukruk, V.V.: Nanotribological properties of organic boundary lubricants: Langmuir films versus self-assembled monolayers. J Tribol-Trans ASME 120, 489–495 (1998)
- Zhang, L., Leng, Y., Jiang, S.: Tip-based hybrid simulation study of frictional properties of self-assembled monolayers: effects of chain length, terminal group, scan direction, and scan velocity. Langmuir 19, 9742–9747 (2003)
- Tsukruk, V.V., Everson, M.P., Lander, L.M., Brittain, W.J.: Nanotribological properties of composite molecular films: C60 anchored to a self-assembled monolayer. Langmuir 12, 3905–3911 (1996)



66 Page 10 of 11 Tribology Letters (2022) 70:66

- van der Vegte, E.W., Subbotin, A., Hadziioannou, G., Ashton, P.R., Preece, J.A.: Nanotribological properties of unsymmetrical n-dialkyl sulfide monolayers on gold: effect of chain length on adhesion, friction, and imaging. Langmuir 16, 3249–3256 (2000)
- Liu, Y., Evans, D.F., Song, Q., Grainger, D.W.: Structure and frictional properties of self-assembled surfactant monolayers. Langmuir 12, 1235–1244 (1996)
- Weymouth, A.J., Hofmann, T., Giessibl, F.J.: Quantifying molecular stiffness and interaction with lateral force microscopy. Science 343, 1120–1122 (2014)
- Cappella, B., Dietler, G.: Force-distance curves by atomic force microscopy. Surf. Sci. Rep. 34, 1–104 (1999)
- Manzi, S.J., Carrera, S.E., Furlong, O.J., Kenmoe, G.D., Tysoe, W.T.: Prandtl–Tomlinson-type models for molecular sliding friction. Tribol. Lett. 69, 147 (2021)
- Evans, M.G., Polanyi, M.: Some applications of the transition state method to the calculation of reaction velocities, especially in solution. Trans. Faraday Soc. 31, 875–894 (1935)
- Marcus, R.A.: On the theory of oxidation-reduction reactions involving electron transfer I. J. Chem. Phys. 24, 966–978 (1956)
- McDermott, M.T., Green, J.-B.D., Porter, M.D.: Scanning force microscopic exploration of the lubrication capabilities of n-alkanethiolate monolayers chemisorbed at gold: structural basis of microscopic friction and wear. Langmuir 13, 2504–2510 (1997)
- Kiely, J.D., Houston, J.E.: Contact hysteresis and friction of alkanethiol self-assembled monolayers on gold. Langmuir 15, 4513–4519 (1999)
- Joyce, S.A., Thomas, R.C., Houston, J.E., Michalske, T.A., Crooks, R.M.: Mechanical relaxation of organic monolayer films measured by force microscopy. Phys. Rev. Lett. 68, 2790–2793 (1992)
- Salmeron, M., Neubauer, G., Folch, A., Tomitori, M., Ogletree, D.F., Sautet, P.: Viscoelastic and electrical properties of selfassembled monolayers on gold (111) films. Langmuir 9, 3600– 3611 (1993)
- 27. Persson, B.N.J.: Sliding friction. North-Holland, Amsterdam (1999)
- Sasaki, N., Tsukada, M., Fujisawa, S., Sugawara, Y., Morita, S.: Theoretical analysis of atomic-scale friction in frictional-force microscopy. Tribol. Lett. 4, 125–128 (1998)
- Furlong, O.J., Manzi, S.J., Pereyra, V.D., Bustos, V., Tysoe, W.T. Kinetic Monte Carlo theory of sliding friction. Phys. Rev. B 80 (2009).
- Müser, M.: Velocity dependence of kinetic friction in the Prandtl– Tomlinson model. Phys. Rev. B 84, 125419 (2011)
- Gnecco, E., Roth, R., Baratoff, A.: Analytical expressions for the kinetic friction in the Prandtl–Tomlinson model. Phys. Rev. B 86, 035443 (2012)
- Manzi, S., Tysoe, W., Furlong, O.: Temperature dependences in the tomlinson/prandtl model for atomic sliding friction. Tribol. Lett. 55, 363–369 (2014)
- Campen, S., Green, J.H., Lamb, G.D., Spikes, H.A.: In situ study of model organic friction modifiers using liquid cell AFM; saturated and mono-unsaturated carboxylic acids. Tribol. Lett. 57, 18 (2015)
- 34. De Barros Bouchet, M.I., Martin, J.M., Forest, C., le Mogne, T., Mazarin, M., Avila, J., et al.: Tribochemistry of unsaturated fatty acids as friction modifiers in (bio)diesel fuel. RSC Adv. 7, 33120–33131 (2017)
- Hardy, W.B., Doubleday, I.: Boundary lubrication. The paraffin series. Proc. R. Soc. Lond. Ser. A 100, 550–574 (1922)
- Jahanmir, S.: Chain length effects in boundary lubrication. Wear 102, 331–349 (1985)
- 37. Hirayama, T., Kawamura, R., Fujino, K., Matsuoka, T., Komiya, H., Onishi, H.: Cross-sectional imaging of boundary lubrication

- layer formed by fatty acid by means of frequency-modulation atomic force microscopy. Langmuir **33**, 10492–10500 (2017)
- 38. Spikes, H.: Friction modifier additives. Tribol. Lett. **60**, 5 (2015)
- Bavisotto, R., Rana, R., Hopper, N., Olson, D., Tysoe, W.T.: Adsorption and reaction pathways of 7-octenoic acid on copper. Phys. Chem. Chem. Phys. 23, 5834–5844 (2021)
- Bavisotto, R., Rana, R., Hopper, N., Hou, K., Tysoe, W.T. Influence of the terminal group on the thermal decomposition reactions of carboxylic acids on copper. Phys. Chem. Chem. Phys. (2021).
- Bavisotto, R., Rana, R., Hopper, N., Tysoe, W.T.: Structure and reaction pathways of octanoic acid on copper. Surf. Sci. 711, 121875 (2021)
- Immaraporn, B., Ye, P., Gellman, A.J.: The transition state for carboxylic acid deprotonation on Cu(100). J. Phys. Chem. B 108, 3504–3511 (2004)
- Parker, B., Immaraporn, B., Gellman, A.J.: Carboxylic acid deprotonation on the Ag(110) and Ag(111) surfaces. Langmuir 17, 6638–6646 (2001)
- Dubois, L.H., Ellis, T.H., Zegarski, B.R., Kevan, S.D.: New insights into the kinetics of formic acid decomposition on copper surfaces. Surf. Sci. 172, 385–397 (1986)
- Sexton, B.A., Hughes, A.E., Avery, N.R.: A spectroscopic study of the adsorption and reactions of methanol, formaldehyde and methyl formate on clean and oxygenated Cu(110) surfaces. Surf. Sci. Lett. 155, A268 (1985)
- Ying, D.H.S., Robert, J.M.: Thermal desorption study of formic acid decomposition on a clean Cu(110) surface. J. Catal. 61, 48–56 (1980)
- Stone, P., Poulston, S., Bennett, R.A., Price, N.J., Bowker, M.: An STM, TPD and XPS investigation of formic acid adsorption on the oxygen-precovered c(6×2) surface of Cu(110). Surf. Sci. 418, 71–83 (1998)
- Bowker, M., Madix, R.J.: The adsorption and oxidation of acetic acid and acetaldehyde on Cu(110). Appl. Surf. Sci. 8, 299–317 (1981)
- Lin, H.-P., Liu, Y.-F., Liu, Y.-X., Yang, Z.-X., Lin, J.-L.: Surface reaction mechanisms: 3-bromopropanoic and 2-bromopropanoic acids on Cu(100) and O/Cu(100). The Journal of Physical Chemistry C 125, 4567–4579 (2021)
- Cheng, H., Hu, Y.: Influence of chain ordering on frictional properties of self-assembled monolayers (SAMs) in nano-lubrication. Adv. Coll. Interface. Sci. 171–172, 53–65 (2012)
- Guo, L.-Y., Zhao, Y.-P.: Effect of chain length of self-assembled monolayers on adhesion force measurement by AFM. J. Adhes. Sci. Technol. 20, 1281–1293 (2006)
- Bhushan, B., Liu, H.: Nanotribological properties and mechanisms of alkylthiol and biphenyl thiol self-assembled monolayers studied by AFM. Phys. Rev. B 63, 245412 (2001)
- Fry, B.M., Moody, G., Spikes, H.A., Wong, J.S.S.: Adsorption of organic friction modifier additives. Langmuir 36, 1147–1155 (2020)
- Rana, R., Bavisotto, R., Hou, K., Tysoe, W.T.: Surface chemistry at the solid–solid interface: mechanically induced reaction pathways of C8 carboxylic acid monolayers on copper. Phys. Chem. Chem. Phys. 23, 17803–17812 (2021)
- Rana, R., Bavisotto, R., Hopper, N., Tysoe, W.T.: Inducing highenergy-barrier tribochemical reaction pathways; acetic acid decomposition on copper. Tribol. Lett. 69, 32 (2021)
- Lio, A., Charych, D.H., Salmeron, M.: Comparative atomic force microscopy study of the chain length dependence of frictional properties of alkanethiols on gold and alkylsilanes on mica. J. Phys. Chem. B 101, 3800–3805 (1997)
- Xiao, X., Hu, J., Charych, D.H., Salmeron, M.: Chain length dependence of the frictional properties of alkylsilane molecules self-assembled on mica studied by atomic force microscopy. Langmuir 12, 235–237 (1996)



Tribology Letters (2022) 70:66 Page 11 of 11 **6**

- Lee, S., Puck, A., Graupe, M., Colorado, R., Shon, Y.-S., Lee, T.R., et al.: Structure, wettability, and frictional properties of phenyl-terminated self-assembled monolayers on gold. Langmuir 17, 7364–7370 (2001)
- Huo, L., Du, P., Zhou, H., Zhang, K., Liu, P.: Fabrication and tribological properties of self-assembled monolayer of n-alkyltrimethoxysilane on silicon: effect of SAM alkyl chain length. Appl. Surf. Sci. 396, 865–869 (2017)
- Nakano, M., Ishida, T., Numata, T., Ando, Y., Sasaki, S.: Alkyl Chain Length Effect on Tribological Behavior of Alkanethiol Self-Assembled Monolayers on Au. Jpn. J. Appl. Phys. 42, 4734

 –4738 (2003)
- Mariscal, R., Maireles-Torres, P., Ojeda, M., Sadaba, I., Lopez Granados, M.: Furfural: a renewable and versatile platform molecule for the synthesis of chemicals and fuels. Energy Environ. Sci. 9, 1144–1189 (2016)
- Leggett, G.J.: Friction force microscopy of self-assembled monolayers: probing molecular organisation at the nanometre scale. Anal. Chim. Acta 479, 17–38 (2003)
- 63. Gao, F., Furlong, O., Kotvis, P.V., Tysoe, W.T.: Pressure dependence of shear strengths of thin films on metal surfaces measured in ultrahigh vacuum. Tribol. Lett. **31**, 99–106 (2008)
- Furlong, O.J., Miller, B.P., Tysoe, W.T.: Shear-induced surfaceto-bulk transport at room temperature in a sliding metal-metal interface. Tribol. Lett. 41, 257–261 (2011)
- Rana, R., Long, D., Kotula, P., Xu, Y., Olson, D., Galipaud, J., et al.: Insights into the Mechanism of the Mechanochemical Formation of Metastable Phases. ACS Appl. Mater. Interfaces (2021).
- Kaltchev, M., Thompson, A.W., Tysoe, W.T.: Reflection-absorption infrared spectroscopy of ethylene on palladium (111) at high pressure. Surf. Sci. 391, 145–149 (1997)
- 67. Kauzmann, W., Eyring, H.: The viscous flow of large molecules. J. Am. Chem. Soc. 62, 3113–3125 (1940)
- Kincaid, J.F., Eyring, H., Stearn, A.E.: The theory of absolute reaction rates and its application to viscosity and diffusion in the liquid state. Chem. Rev. 28, 301–365 (1941)
- Seah, M.P., Dench, W.A.: Quantitative electron spectroscopy of surfaces: A standard data base for electron inelastic mean free paths in solids. Surf. Interface Anal. 1, 2–11 (1979)
- Briggs, B., Seah, M.P.: Practical Surface Analysis: Auger and X-ray Photoelectron Spectroscopy. John Wiley and Sons, New York (1996)

- Carlson, T.A., McGuire, G.E.: Study of the x-ray photoelectron spectrum of tungsten—tungsten oxide as a function of thickness of the surface oxide layer. J. Electron Spectrosc. Relat. Phenom. 1, 161–168 (1972)
- Strohmeier, B.R.: An ESCA method for determining the oxide thickness on aluminum alloys. Surf. Interface Anal. 15, 51–56 (1990)
- Evans, S.D., Goppert-Berarducci, K.E., Urankar, E., Gerenser, L.J., Ulman, A., Snyder, R.G.: Monolayers having large in-plane dipole moments: characterization of sulfone-containing selfassembled monolayers of alkanethiols on gold by Fourier transform infrared spectroscopy, x-ray photoelectron spectroscopy and wetting. Langmuir 7, 2700–2709 (1991)
- Sellers, H., Ulman, A., Shnidman, Y., Eilers, J.E.: Structure and binding of alkanethiolates on gold and silver surfaces: implications for self-assembled monolayers. J. Am. Chem. Soc. 115, 9389–9401 (1993)
- Ulman, A.: Formation and structure of self-assembled monolayers. Chem. Rev. 96, 1533–1554 (1996)
- Wood, K.A., Snyder, R.G., Strauss, H.L.: Analysis of the vibrational bandwidths of alkane–urea clathrates. J. Chem. Phys. 91, 5255–5267 (1989)
- Chandross, M., Grest, G.S., Stevens, M.J.: Friction between alkylsilane monolayers: molecular simulation of ordered monolayers. Langmuir 18, 8392–8399 (2002)
- Tutein, A.B., Stuart, S.J., Harrison, J.A.: Role of defects in compression and friction of anchored hydrocarbon chains on diamond. Langmuir 16, 291–296 (2000)
- Bonner, T., Baratoff, A.: Molecular dynamics study of scanning force microscopy on self-assembled monolayers. Surf. Sci. 377– 379, 1082–1086 (1997)
- Mikulski, P.T., Harrison, J.A.: Packing-density effects on the friction of n-alkane monolayers. J. Am. Chem. Soc. 123, 6873–6881 (2001)

Publisher's Note Springer Nature remains neutral with regard to jurisdictional claims in published maps and institutional affiliations.

Authors and Affiliations

Kaiming Hou³ · Robert Bavisotto³ · Sergio Javier Manzi¹ · Eliseo Joaquín Perez¹ · Octavio Javier Furlong¹ · Peter Kotvis³ · Germaine Djuidje Kenmoe^{2,3} · Wilfred T. Tysoe³

- ¹ Instituto de Física Aplicada (INFAP), CONICET-Universidad Nacional de San Luis, Chacabuco 917, 5700 San Luis, Argentina
- Department of Physics, Faculty of Science, University of Yaounde 1, P.O. Box 812, Yaounde, Cameroon
- Department of Chemistry and Biochemistry, and Laboratory for Surface Studies, University of Wisconsin-Milwaukee, Milwaukee, WI 53211, USA

